

Multiplet resonance-fluorescence spectra of a three-level medium (sodium vapor) in intense laser radiation

A. G. Leonov, A. A. Pantelev, A. N. Starostin, and D. I. Chekhov

Moscow Physicotechnical Institute, 111700 Dolgoprudnyi, Moscow Region, Russia

(Submitted 26 January 1994)

Zh. Eksp. Teor. Fiz. **105**, 1536–1558 (June 1994)

We report the first determination of the fluorescence spectra of a dense ($N \sim 10^{15} \text{ cm}^{-3}$) three-level medium in intense laser radiation. We have recorded their multiplet structure, associated with Rabi splitting into three quasilevels of the $3S$ ground state and two excited $3P$ levels of the sodium atom. When the spatial nonuniformity of the laser beam and the absorption of fluorescence photons in the undisturbed sodium vapors are taken into account, the calculated spectra are in good agreement with experiment.

1. INTRODUCTION

The investigation of resonance fluorescence induced by resonant laser radiation is fundamental to understanding the interaction of radiation with matter, and a great deal of attention has been devoted to such investigations over a period of many years. It is well known that when a two-level medium is excited by weak monochromatic light the resonance-fluorescence spectrum is determined by coherent Rayleigh scattering, if the lower level is the ground state.¹ The small parameter in this case is the ratio of the Rabi frequency $\Omega = \mu E_L / \hbar$ (where μ is the dipole moment and E_L is the intensity of the electric field of the laser radiation) to the spontaneous relaxation rate γ or the detuning Δ from resonance. In strong fields $\Omega \gg \gamma$, Δ , however, spontaneous emission in the form of a triplet (Mollow triplet—see Ref. 2) is added to the coherent component of the fluorescence spectrum. We note that Rautian and Sobel'man³ were the first to obtain the resonance-fluorescence spectrum of an intense monochromatic wave for scattering by an open two-level system. Like Mollow's spectrum, their spectrum has the triplet structure.

Mollow assumed that the relaxation of the atomic system is radiative.² Then the fluorescence spectrum is symmetric, even if the frequency of the exciting radiation is detuned from the transition frequency. Mollow⁴ and Carlsten *et al.*⁵ later showed that in a dense medium, because of the strong influence of collisional processes, in the presence of detuning the spectrum becomes asymmetric and the center of gravity of the triplet is displaced in the direction of the resonance-transition frequency. Note that the theoretical models developed in Refs. 2, 4, and 5 are well-confirmed by experiments (see, for example, Refs. 6–8).

The two-level description is often invalid, however, for high laser-beam intensities, such as those employed recently in experiments on the investigation of the resonance interaction of laser radiation with real atomic systems (for example, alkali-metal vapors) because the splitting from the resonance level to the neighboring perturbing levels becomes of the order of the Rabi frequency and the effect

of the latter levels must be taken into account when modeling the fluorescence and scattering processes. In the case of experiments with alkali-metal vapor exposed to radiation whose wavelength is close to that of one of the D lines, this means that the influence of a neighboring level becomes significant when the Rabi frequency Ω is of the order of the doublet splitting δ . For the specific example of sodium vapors, depending on the D line for which the Rabi frequency is calculated, the condition $\Omega \approx \delta$ holds for moderate laser intensities $\mathcal{I} \approx 40\text{--}80 \text{ MW/cm}^2$, typically used in modern experiments.

We reported briefly in Ref. 9 the first experimental observation and theoretical modeling of the fluorescence spectra of a three-level medium. In the present paper the theoretical analysis of the problem and the results of experiments and numerical calculations are discussed in greater detail. The basic equations describing the interaction of an intense monochromatic wave with a three-level atomic system are presented in Sec. 2; the equations are based on the Scully–Lamb atom-photon density matrix formalism.¹⁰ In Sec. 3 the fluorescence spectra of a three-level atom are studied theoretically, and the spectra are interpreted from the standpoint of dressed-atom states. The experimental apparatus is described in Sec. 4, and the experimental results are presented in Sec. 5. Model calculations of fluorescence under actual experimental conditions are presented in Sec. 6.

2. BASIC EQUATIONS

As noted above, the two-level approximation is often found to be inadequate for describing the interaction of intense radiation with atoms of a resonant medium. Thus the interpretation of the results of many experiments on nonlinear scattering of laser radiation and fluorescence in sodium vapors (see, for example, Refs. 9 and 11–13) must include the fact that the laser field effectively interacts simultaneously with the two transitions in the sodium atom $D_1(3^2S_{1/2}\text{--}3^2P_{1/2})$ and $D_2(3^2S_{1/2}\text{--}3^2P_{3/2})$, since under these the Rabi frequency Ω is not small compared to the doublet splitting δ . This corresponds to a V -type interac-

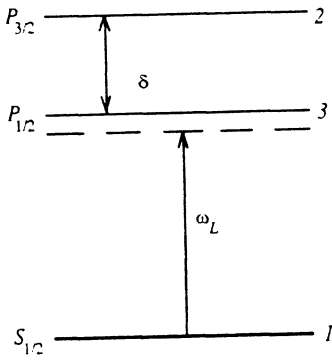


FIG. 1.

tion of the electromagnetic radiation with a three-level system. It is this interaction that we shall consider in the present work, and we assume for definiteness that the parameters of the atomic subsystem correspond to the sodium doublet (see Fig. 1).

The fluorescence spectra of the resonant two-level medium in a strong field have been calculated by different methods by many workers (see, the review Ref. 14 and the bibliography provided there). In the present paper we employ the atom-photon density matrix formalism¹⁰ in order to find the fluorescence spectra of a three-level system. This formalism was first used by Baklanov in order to calculate resonance-fluorescence spectra.¹⁵ The method was developed by Sargent *et al.* in order to describe multiwave interaction processes.^{16,17} We employ the approach used in these works, since the formalism proposed there is the most convenient formalism for extension to the multilevel case.

Assuming a rotating wave and a dipole interaction, we represent the Hamiltonian of the system under consideration in this case as a sum

$$H = H_0 + H_r + H_L + H_q, \quad (1)$$

where H_0 is the Hamiltonian of the unperturbed atomic subsystem, H_r is the Hamiltonian of the radiation field, and H_L and H_q describe the interaction of the atoms with the laser wave and with the quantized radiation field.

The Hamiltonians can be represented as follows (in rad/sec):

$$H_0 = \Delta R_z + \delta R_D, \quad H_r = \sum \nu_j a_j^\dagger a_j, \quad (2)$$

$$H_L = \sum_{m=2,3} (V_m R_{1m}^+ + V_m^* R_{m1}^-),$$

$$H_q = \sum_{j,m} (g_{mj} R_{1m}^+ a_j U_j + \text{h.c.}),$$

where $\Delta = (\omega_{21} + \omega_{31})/2 - \omega_L$; $\nu_j = \omega_j - \omega_L$, where ω_j is the frequency of photons with wave vector \mathbf{k}_j ; a_j^\dagger and a_j are creation and annihilation operators for photons of the j th mode; $U_j = U_j(\mathbf{r})$ is the spatial mode factor;

$$V_m = -\mu_{m1} E_L U_L / 2\hbar \quad (m=2,3),$$

where μ_{21} , μ_{23} , ω_{21} , and ω_{31} are, respectively, the matrix elements of the dipole moment and the unperturbed resonance frequencies of the $D_2(3^2S_{1/2}-3^2P_{3/2})$ and $D_1(3^2S_{1/2}-3^2P_{1/2})$ transitions in the sodium atom; $\delta = \omega_{21} - \omega_{31}$ is the doublet splitting; ω_L and E_L are the frequency and amplitude of the electric-field intensity of the monochromatic wave; and

$$g_{jm} = -i\mu_{m1} \sqrt{2\pi\omega_j / \hbar \mathcal{V}}$$

is the coupling constant of the j th mode with the transition $1 \rightarrow m$ (\mathcal{V} is the quantization volume). The R matrices are the three-dimensional extension of the 2×2 Pauli matrices to the three-level system displayed in Fig. 1. They satisfy the following commutation relations:

$$[R_z, R_{1m}^+] = (-1)^m 2R_{1m}^+, \quad [R_z, R_{m1}^-] = (-1)^{m+1} R_{m1}^-,$$

$$[R_D, R_{1m}^+] = (-1)^m R_{1m}^+, \quad [R_D, R_{m1}^-] = (-1)^{m+1} R_{m1}^-,$$

$$(m=2,3), \quad (3)$$

and the action on the eigenfunctions of the atomic subsystem is determined by the expressions

$$R_{1m}^+ |m'\rangle = |m\rangle \delta_{1m'}, \quad R_{m1}^- |m'\rangle = |1\rangle \delta_{mm'}, \quad (4)$$

where $\delta_{mm'}$ is the Kronecker delta function.

The components of the atomic density matrix ρ are determined as follows:

$$\rho_{1m} = \langle R_{1m}^+ \rho \rangle, \quad \rho_{m'm} = \langle R_{m1}^- R_{1m}^+ \rho \rangle,$$

$$\rho_{m1} = \langle R_{m1}^- \rho \rangle, \quad \rho_{11} = \langle R_{1m}^- R_{m1}^+ \rho \rangle \delta_{mm'}. \quad (5)$$

The equation of motion for the atom-photon density matrix ρ_{a-ph} has the form

$$i\dot{\rho}_{a-ph} = [H; \rho_{a-ph}] + i\Gamma(\rho_{a-ph}), \quad (6)$$

where the operator $\Gamma(\rho_{a-ph})$ describes relaxation processes. Contracting the photon variables in Eq. (6) we obtain an equation for the atomic density matrix ρ and, conversely, taking the trace over the atomic states we obtain an equation for the photon field operator P . Following Refs. 16 and 17, we represent the atomic-photon density matrix in the factorized form $\rho_{a-ph} = P \cdot \rho$. Neglecting radiation trapping and saturation of the atomic subsystem by quantized fields (which, of course, are assumed to be small) we obtain the following equation for the atomic density matrix:

$$i\dot{\rho} = [H_0 + H_1, \rho] + i\Gamma(\rho), \quad (7)$$

or

$$i\dot{\rho} = \mathbf{L}\rho, \quad (8)$$

where the transposed column of the components of the density matrix has the form

$$\rho^T = (\rho_{11}, \rho_{22}, \rho_{33}, \rho_{12}, \rho_{21}, \rho_{13}, \rho_{31}, \rho_{32}, \rho_{23}),$$

and

$$\mathbf{L} = \begin{pmatrix} 0 & i\gamma & i\gamma & -V_2 & V_2^* & -V_3 & V_3^* & 0 & 0 \\ 0 & -i\gamma_2 & i\nu_c & V_2 & -V_2^* & 0 & 0 & 0 & 0 \\ 0 & i\nu_c & -i\gamma_3 & 0 & 0 & V_3 & -V_3^* & 0 & 0 \\ -V_2^* & V_2^* & 0 & -\Delta_{21}^* & 0 & 0 & 0 & V_3^* & 0 \\ V_2 & -V_2 & 0 & 0 & \Delta_{21} & 0 & 0 & 0 & -V_3 \\ -V_3^* & 0 & V_3^* & 0 & 0 & -\Delta_{31}^* & 0 & 0 & V_2^* \\ V_3 & 0 & -V_3 & 0 & 0 & 0 & \Delta_{31} & -V_2 & 0 \\ 0 & 0 & 0 & V_3 & 0 & 0 & -V_2^* & -\tilde{\delta}^* & i\tilde{\nu}_c \\ 0 & 0 & 0 & 0 & -V_3^* & V_2 & 0 & i\tilde{\nu}_c & \tilde{\delta} \end{pmatrix}.$$

Here $\Delta_{m1} = \Delta_m - i\gamma_{m1}$, $\tilde{\delta} = \delta - i\gamma_{23}$, and $\Delta_m = \omega_{m1} - \omega_L$. Since the atomic subsystem is closed, Eq. (8) must be supplemented by the condition $\text{Sp}(\rho) = 1$.

In the calculations it is assumed that the longitudinal relaxation constants γ_m include the spontaneous relaxation rate γ and the collisional mixing ν_c of the levels. The transverse relaxation constants γ_{mk} take into account, besides these processes, pressure broadening by the atomic vapor and pressure broadening by the buffer gas. The values of these constants were taken from Refs. 18–20.

Although the fields considered in the present work are assumed to be quite strong, the dependence of the relaxation constants on the intensity of the pump wave²¹ is neglected. Estimates show that this is justified for the range of values of the parameters of the experiment discussed below.

The thermal motion of the atoms is also neglected in the calculations. The characteristic Rabi frequencies for this problem are much higher than the Doppler half-width, so that taking into account the thermal motion does not significantly alter the spectra but merely broadens the peaks somewhat. The importance of this factor is also reduced by the presence of significant detuning (see Sec. 5) from resonances.

It was shown in Refs. 16 and 17 that the equation for the photon field operator P can be represented as follows:

$$\dot{P} = \mathcal{A}(a^+Pa - Paa^+) + \mathcal{B}(aPa^+ - a^+aP) + \text{h.c.} \quad (9)$$

In the present paper we investigate the resonance-fluorescence spectra, and in the experimental geometry considered the four-wave interaction processes^{11–13} are unimportant. We shall consider the interaction of the three-level medium with an intense incident wave and the quantized mode orthogonal to this wave, so that here and below the index j [see Eq. (2)] is dropped.

We are mainly interested in the photon occupation numbers n , defined by the relation $n = \langle a^+aP \rangle$. The equation of motion for n follows from Eq. (9) and has the form

$$\frac{d}{dt}n = (\mathcal{A} - \mathcal{B})n + A + \text{c.c.} \quad (10)$$

The free term $A = \mathcal{A} + \mathcal{A}^*$ in Eq. (9) describes spontaneous emission and determines the resonance-

fluorescence spectrum, and the coefficient $\alpha = \mathcal{A} - \mathcal{B} + \text{c.c.}$ determines the photon absorption (amplification).

We have the following expressions for the coefficients \mathcal{A} and \mathcal{B} :

$$\begin{aligned} \mathcal{A} = & -i\bar{N}[(g_2\rho_{12} + g_3\rho_{13})(g_2^*m_{15} + g_3^*m_{17}) + (g_2\rho_{22} \\ & + g_3\rho_{23}) \times \\ & (g_2^*m_{55} + g_3^*m_{57}) + (g_2\rho_{32} + g_3\rho_{33}) \\ & \times (g_2^*m_{75} + g_3^*m_{77})], \end{aligned} \quad (11)$$

$$\begin{aligned} \mathcal{B} = & -i\bar{N}[\rho_{12}[|g_2|^2m_{25} + g_2g_3^*(m_{85} + m_{27}) + |g_3|^2m_{87}] \\ & + \rho_{11}[|g_2|^2m_{55} + g_2g_3^*(m_{75} + m_{57}) + |g_3|^2m_{77}] \\ & + \rho_{13}[|g_2|^2m_{95} + g_2g_3^*(m_{35} + m_{97}) + |g_3|^2m_{37}], \end{aligned} \quad (12)$$

where ρ_{jk} are the stationary solutions of the system (8), $m_{jk} = \det M_{jk} / \det \mathbf{M}$, and M_{jk} is a minor of the matrix $\mathbf{M} = \mathbf{L} - \nu\mathbf{I}$ (where \mathbf{I} is a unit matrix), $\nu = \omega - \omega_L$, and \bar{N} is the number of interacting atoms.

It is well known^{1,2} that for a closed atomic subsystem, i.e., when the lower state is the ground state, the resonance-fluorescence spectrum contains an undisplaced (or elastic) component, which corresponds to scattering of the incident wave with no change in frequency, and a displaced (inelastic) component, corresponding to scattering with a change in photon frequency. We express the fluorescence spectrum in the form

$$A = A^{el} + A^{inel}, \quad (13)$$

where A^{el} describes the undisplaced component and, in the case at hand, has the form

$$A^{el} = 2\pi\bar{N}|g_2\rho_{12} + g_3\rho_{13}|^2\delta(\nu), \quad (14)$$

where $\delta(\nu)$ is a Dirac delta function.

The expressions obtained for the spectra are a generalization of the emission and absorption spectra of a two-level atom in the field of an intense wave^{2,4,22} to the case of the three-level system displayed in Fig. 1. The results of Refs. 2 and 4 follow from the expression (11) in the case

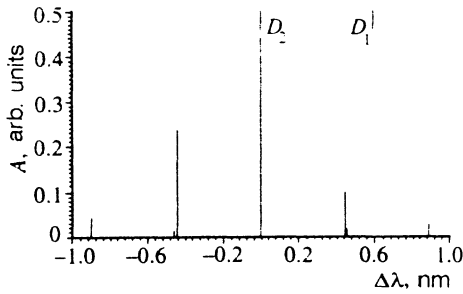


FIG. 2. Spontaneous emission spectrum of a three-level atom in the field of an intense laser wave in resonance ($\Delta\lambda_L=0$) with the transition D_2 in the case of purely radiative relaxation of the atomic subsystem; $\mathcal{L}=20$ MW/cm².

when the wave is tuned near one of the transitions ($\Delta_m \ll \delta$), and its intensity, though it can saturate the nearest transition, must be quite low: $V_m \ll \delta$.

3. FLUORESCENCE SPECTRA AND THEIR ANALYSIS

The spontaneous-emission spectra and the photon absorption coefficient in the presence of laser radiation, calculated in accordance with the expressions (11) and (12), are presented in Figs. 2 and 3 for the case of purely radiative damping of the atomic subsystem and correspond to the intensity $\mathcal{L}=20$ MW/cm² of the incident wave which is in exact resonance with the D_2 transition of the sodium atom: $\Delta\lambda_L=0$, $\Delta\lambda_L = \lambda_{D_2} - \lambda_L$ ($\lambda_{D_2} = 588.995$ nm is the wavelength of the D_2 line). As follows from the figures, the spectra contain seven peaks, two pairs of which, with $\Delta\lambda \approx \pm 0.445$ nm ($\Delta\lambda = \lambda_{D_2} - \lambda$, where λ is the wavelength of the scattered photon), are almost identical and virtually indistinguishable in the plots. A significant difference from the spectra of a two-level atom^{2,22} is the asymmetry of the computed spectra: very strong for the photon absorption (amplification) coefficient and smaller for the emission spectra. Under these conditions the ratios of the widths of the peaks are approximately as follows: 2:2:1.5:1:1.5:2:2, where the width of the central peak is unity.

Figure 4 displays the calculated fluorescence spectra for the same intensity of the laser radiation, whose wavelength is detuned from the D_2 transition ($\Delta\lambda_L=0.21$ nm) in the radiative-relaxation regime (Fig. 4a) and in the col-

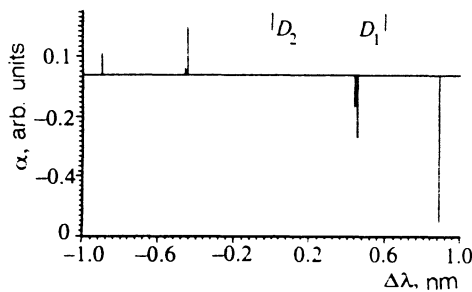


FIG. 3. Absorption spectrum of a three-level atom in the field of an intense laser wave under the conditions of Fig. 2.

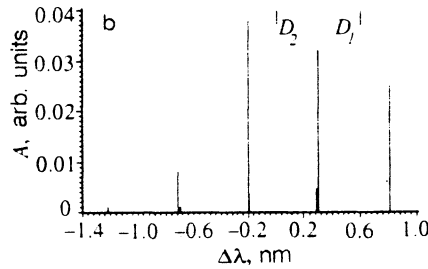
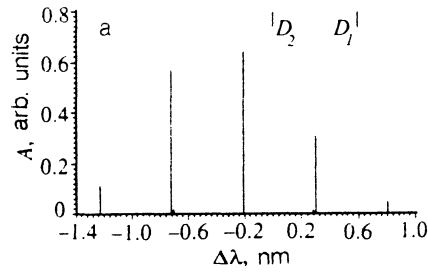


FIG. 4. Spontaneous emission spectrum of a three-level atom in the field on an intense laser wave detuned from the D_2 line by $\Delta\lambda_L=0.21$ nm in (a) the radiative relaxation regime and (b) the strong-collision regime with atom density $N=2.3 \cdot 10^{15}$ cm⁻³; $\mathcal{L}=20$ MW/cm².

lisional regime ($N=2.3 \cdot 10^{15}$ cm³; Fig. 4b). It is evident from this figure that, just as for the spectra of a two-level atom,^{4,5} collisions redistribute the scattering in the direction of the lines of the transitions.

We note that Figs. 2 and 4 display the spectra of only the inelastic component of fluorescence. The contribution of the undisplaced component in strong fields ($\Omega \sim \delta$) is small, just as in the case of a two-level atom.²

The absorption and emission processes in an atom in the presence of intense laser radiation can be interpreted as transitions between quasienergy levels of the system which includes the three-level atom under consideration and the field of the intense electromagnetic wave (i.e., between states of a "dressed" atom²³). The quasienergy spectrum of such a system can be obtained from the expressions for the poles of the retarded Green's functions. Using the description developed in Refs. 24 and 25 on the basis of Keldysh's diagrammatic technique for nonequilibrium Green's functions,²⁶ we can derive the following expressions for the retarded functions:

$$G_{11}^r(\varepsilon) = \alpha_2 \alpha_3 / S(\varepsilon), \quad (15)$$

$$G_{22}^r(\varepsilon + \omega_L) = (\alpha_1 \alpha_3 - |V_3|^2) / S(\varepsilon), \quad (16)$$

$$G_{33}^r(\varepsilon + \omega_L) = (\alpha_1 \alpha_2 - |V_2|^2) / S(\varepsilon), \quad (17)$$

where $\alpha_1 = \varepsilon$, $\alpha_j = \varepsilon - \Delta_j$ ($j=2,3$), $S(\varepsilon) = \alpha_1 \alpha_2 \alpha_3 - |V_2|^2 \alpha_3 - |V_3|^2 \alpha_2$.

The quasienergy spectrum of the system consisting of the three-level atom plus the field will be determined by an equation which can likewise be derived by solving the time-dependent Schrodinger equation:²³

$$S(\varepsilon) = (\varepsilon - \varepsilon_1)(\varepsilon - \varepsilon_2)(\varepsilon - \varepsilon_3) = 0. \quad (18)$$

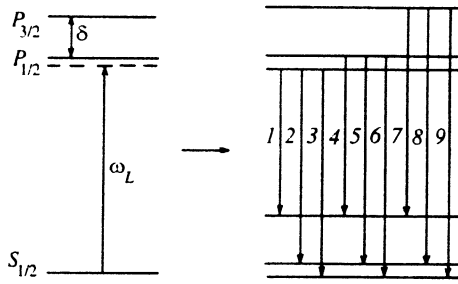


FIG. 5. Splitting and shift of the sodium resonance levels in the field of a strong laser wave. The transitions 3, 5, and 7 describe emission at the laser frequency; transitions 6 and $2-\omega_1^\pm = \omega_L \pm \Omega_1'$; transitions 8 and $4-\omega_2^\pm = \omega_L \pm \Omega_2'$; and transitions 9 and $1-\omega_3^\pm = \omega_L \pm \Omega_3'$.

The roots of this equation ε_k ($k=1, 2$, and 3) are the Rabi frequencies of the oscillations (quasienergies) and they determine the generalized Rabi frequencies of the three-level system:

$$\Omega_j' = |\varepsilon_k - \varepsilon_{k'}|, \quad j=1,2,3, \quad k \neq k'. \quad (19)$$

We note that the approximate solutions of the cubic equation (18) are easily found for sufficiently high intensities ($W \gg \Delta$):

$$\varepsilon_1 \approx \Delta \left(1 + \frac{\delta^2}{3W^2} \right), \quad \varepsilon_{2,3} \approx \frac{1}{2} \left[\Delta \left(1 - \frac{\delta^2}{3W^2} \right) \pm W \right], \quad (20)$$

where $W = \sqrt{\delta^2 + 4|V_2|^2 + 4|V_3|^2}$.

The splitting of the levels of a three-level atom in the field of a strong laser wave is displayed in Fig. 5 and includes three upper and three lower levels. From Fig. 5, transitions between them result in the appearance of three degenerate lines in the scattered spectrum at the frequency $\omega = \omega_L$ as well as six lines whose frequencies are shifted relative to ω_L : $\omega_j^\pm = \omega_L \pm \Omega_j'$. In the limit of low intensity this splitting is described by Raman scattering at frequencies detuned from the laser wave by the amounts $\Omega_1' \simeq |\Delta_2|$, $\Omega_2' \simeq \delta$, and $\Omega_3' \simeq |\Delta_3|$.

It should be noted that the quasienergy structure of the atom can also be found using the approach developed in Sec. 2. Then the quantities Ω_j' are determined by the real part of the eigenvalues of the matrix L which are found from the equation

$$\det(L - \nu I) = \nu F(\nu) = 0, \quad (21)$$

where $F(\nu)$ is a polynomial of degree eight and is a generalization of Mollow's well-known cubic polynomial.² The imaginary parts of the eigenvalues of the matrix L will be determined, however, by the exact widths of the corresponding peaks. The exact solution $\nu=0$ of Eq. (21) with zero line width corresponds to the coherent component, described by the expression (14), of the fluorescence spectrum. Note that $F(\nu)$ satisfies $F(-\nu) = F^*(\nu)$.

For the case corresponding to Mollow's problem,² i.e., when in the radiative relaxation regime the wave is tuned

near one of the transitions, for example, $\Delta_2 \ll \delta$, and its intensity is so high that $V_2 \ll \delta$, the polynomial $F(\nu)$ can be approximated by

$$F(\nu) \approx f(\nu)(\nu + i\gamma) \left(\nu - \delta + \frac{\Omega' - \Delta_2}{2} + \frac{5}{4}i\gamma \right) \times \left(\nu - \delta - \frac{\Omega' + \Delta_2}{2} + \frac{5}{4}i\gamma \right) \left(\nu + \delta - \frac{\Omega' + \Delta_2}{2} + \frac{5}{4}i\gamma \right) \left(\nu + \delta + \frac{\Omega' - \Delta_2}{2} + \frac{5}{4}i\gamma \right), \quad (22)$$

where

$$f(\nu) = (\nu + i\gamma)(\nu + \Delta_2 + i\gamma/2)(\nu - \Delta_2 + i\gamma/2) - 2|V_2|^2(2\nu + i\gamma)$$

is the cubic Mollow polynomial, and

$$\Omega' = \sqrt{\Delta_2^2 + 4|V_2|^2}$$

is the generalized Rabi frequency of the two-level system. The emission spectrum of the atom in this case will actually be determined by the Mollow triplet, since the intensities of the other peaks are found to be negligibly small. The absorption spectrum near the D_2 transition will also be determined by the absorption (amplification) coefficient of the probe signal of the two-level system in the field of an intense electromagnetic wave.²² The absorption spectrum near the D_1 transition changes significantly, however, even though the pump wave essentially does not interact with it: instead of one absorption peak there are two peaks split by Ω' . Their appearance is evidently associated with the splitting of the lower state due to the high-frequency Stark effect on the D_2 transition.

4. EXPERIMENTAL APPARATUS

The experiments were performed on an apparatus consisting of a frequency-tunable dye laser, a heated cell holding the sodium vapor, and diagnostic instrumentation (see Fig. 6). The construction of the heated cell was similar to that described in Ref. 27 and made it possible to produce a 1.5 cm high cylindrical column of sodium vapor with density 10^{13} – 10^{16} cm⁻³. Prior to the experiments the cell was evacuated to a pressure of 10^{-5} torr, filled with inert gas (argon) at a pressure of ~ 0.3 – 5 torr, and heated up to the required temperature.

The tunable dye laser was excited by the second-harmonic radiation of a YAG:Nd³⁺ laser, operating with a pulse repetition frequency of 10 Hz, and generated linearly polarized radiation with energy E up to 6 mJ with spectral width 0.008 nm and pulse length $\tau = 18$ nsec. The laser beam was focused with a lens of focal length 45 cm into the center of the cell; the beam radius $r_{1/2}$ at half-maximum of the energy spectrum in this region, measured with a linear photodiode array in a cold cell (i.e., in the absence of a vapor), was equal to 0.3 mm (see Fig. 7). Note that in the

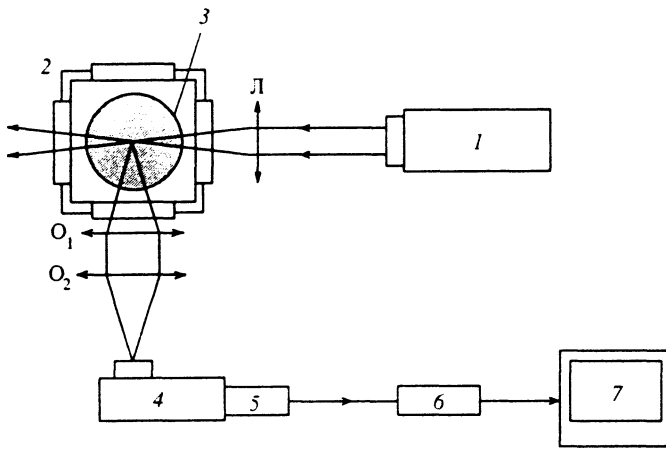


FIG. 6. Experimental arrangement: 1—tunable dye laser, 2—heated cell, 3—disk of sodium vapors, 4—monochromator, 5—FÉU-84 photomultiplier, 6—gated V9-5 voltmeter, 7—personal computer, L—focusing lens; O₁ and O₂—objectives of the projection system.

following discussion of the experimental data the laser radiation intensity is the quantity calculated from the formula $\mathcal{I} = E\tau S$, where $S = \pi r_{1/2}^2$.

The density N of sodium atoms and the radial density distribution $N(R)$ in the cell were reconstructed by means of Abel transforms, using the cylindrical symmetry of the vapor, from measurements of the quantity

$$N'(x) = \int N(x,y) dy$$

by the method of Rozhdestvenskii hooks. The measurement scheme is displayed in Fig. 8. In order to obtain the hooks the sodium vapor column was placed in one arm of a Michelson interferometer, formed by the nontransmitting mirrors $M1$ and $M2$ and a half-transmitting plate P , illuminated by an auxiliary wide-band ($\Delta\lambda \approx 6$ nm) pulsed dye laser (rhodamine 6G solution in ethanol). The maximum of the lasing spectrum of the laser was displaced into the region of the sodium D lines by adjusting the dye concentration. The interference pattern was projected onto the input slit of a DFS-452 diffraction spectrograph, in whose focal plane the hooks were observed. The spatial resolution

of the recording system was limited by the diameter of the laser beam, which in the present experiments was equal to 1 mm. By moving the cell along the x axis it was possible to illuminate the sodium vapor along different chords and thus to construct the function $N'(x)$, which was then smoothed by approximating the experimental data by the method of least squares using a cubic polynomial. The sodium-vapor density distribution obtained by Abel-transforming the polynomial over the radius of the cell is shown in Fig. 9 for a particular heater power. It should be noted that, as the measurements showed, the diameter of the vapor column and the shape of the distribution curve were virtually independent of the heating temperature and the pressure of the buffer gas. In what follows, the sodium vapor density will be the value of N at the maximum of the distribution $N(R)$ reconstructed in the manner described above.

The sodium-vapor fluorescence produced by the laser radiation was collected from the center of the cell in the direction perpendicular to the axis of the laser beam by means of two objectives, which formed an image of the bright region on the input slit of the diffraction monochro-

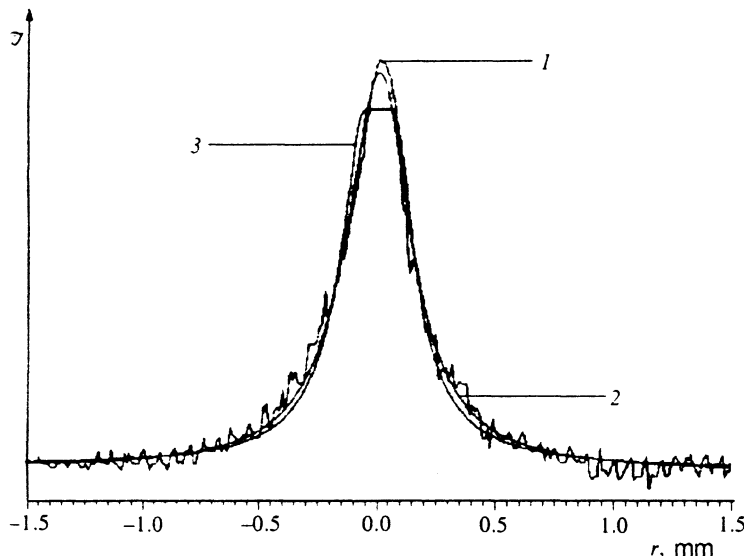


FIG. 7. Laser radiation intensity distribution over the cross section of the laser beam. 1—Experiment, 2, 3—least-squares approximation of the distribution by Lorentzian (23) and Gaussian (24) functions.

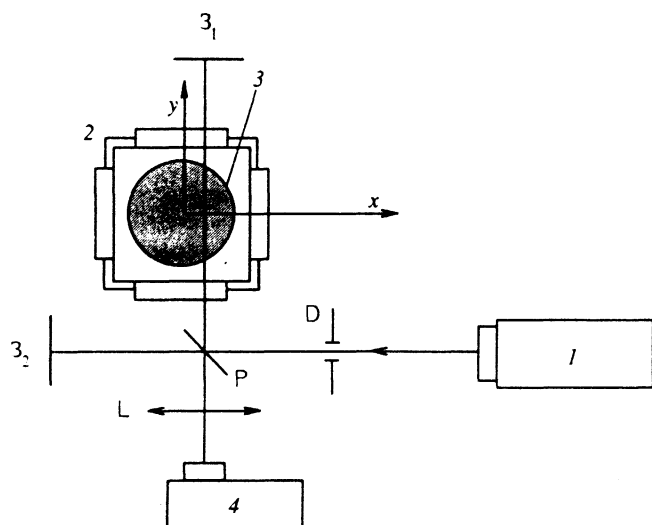


FIG. 8. Experimental arrangement used to measure the radial distribution of the sodium vapor density in the cell. 1—Wideband dye laser, 2—heated cell, 3—disk of sodium vapors, 4—DFS-452 spectrograph, L—focusing lens, M1 and M2—interferometer mirrors, P—beamsplitting plate, D—diaphragm.

mator (1200 lines/mm). An FÉU-84 photomultiplier was placed behind this input slit. The signal from the photomultiplier was recorded with a gated voltmeter at the time corresponding to the maximum of the pulse from the dye laser. It should be noted that the lasing intensity remained virtually constant within the gate (4 nsec). In order to obtain the fluorescence spectrum the transmission wavelength of the monochromator was automatically scanned near the D_1 and D_2 lines of sodium. The spectral resolution of this measuring system was 0.02 nm. In performing the experiments special attention was devoted to decreasing the background illumination of the recording apparatus by the scattered radiation of the exciting laser. In our exper-

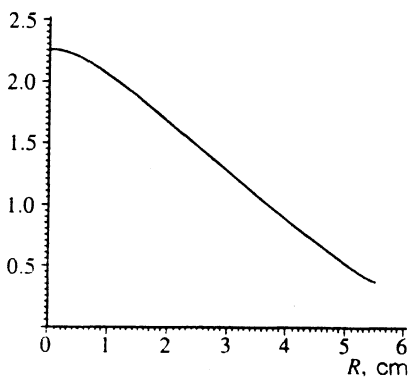
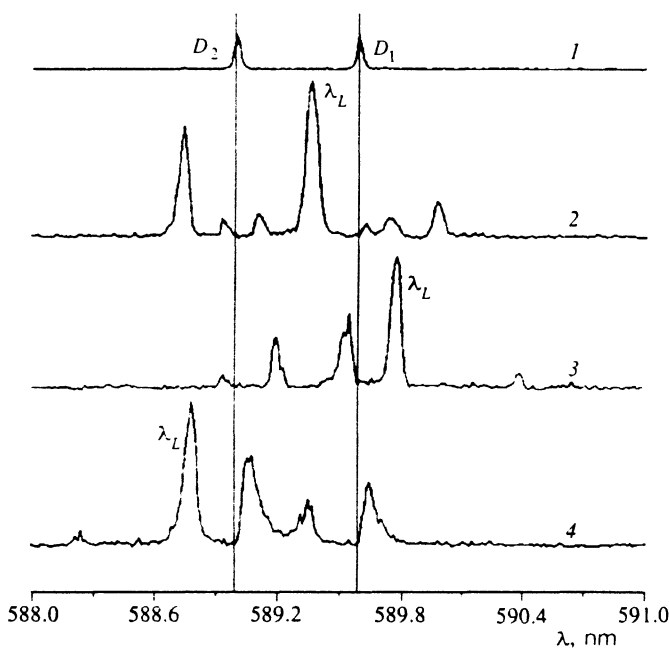


FIG. 9. Sodium vapor density as a function of the cell radius R .

iments the intensity of the background signal at the laser frequency was less than 10% of the intensity of the fluorescence line in all measurement regimes. This was checked by measuring the background intensity with and without vapor, but with large detuning (~ 20 nm) of the laser frequency from resonance.

5. EXPERIMENTAL RESULTS

The sodium-vapor fluorescence spectra, recorded in the experiments and excited by an intense laser beam, are displayed in Fig. 10. It is evident from the data presented in these spectra that if the laser wavelength λ_L falls between the D lines, then the fluorescence spectrum contains seven components. This reflects the splitting of the three-level medium in a strong laser field, described above. If, however, λ_L lies outside this range, then only five components are observed in the spectra, and the characteristic feature of these components is that with high-frequency detuning of the laser radiation from the D_2 line the most intense fluorescence lines lie at frequencies below the laser

FIG. 10. Measured fluorescence spectra of sodium vapors with detunings $\Delta\lambda_L = -0.37$ nm (2), $\Delta\lambda_L = -0.79$ nm (3), and $\Delta\lambda_L = 0.21$ nm (4). $N = 2.3 \cdot 10^{15}$ cm $^{-3}$, $\mathcal{I} = 20$ MW/cm 2 ; 1—calibration spectrum of the sodium lamp.

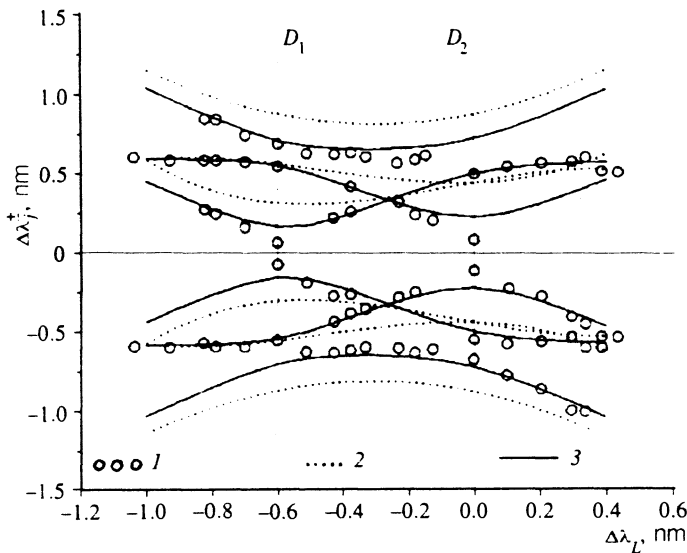


FIG. 11. Measured (1) and computed (2, 3) shifts $\Delta\lambda_j^\pm$ of the components of the fluorescence spectrum of sodium vapors. $N=2.3 \cdot 10^{15} \text{ cm}^{-3}$; 1, 2— $\mathcal{I}=20 \text{ MW/cm}^2$; 3— $\mathcal{I}=5 \text{ MW/cm}^2$.

frequency; the opposite is true for low-frequency detuning from the D_1 line. The intensity of the two other components in this case is, however, apparently very low (this is confirmed by the calculations; see the discussion below) and is at the noise level. The asymmetry found in the fluorescence spectra for high buffer-gas and sodium-vapor pressures is associated, as we have already mentioned above (see, also Refs. 4 and 5), with the large role of collisions.

It should be noted, however, that the recorded fluorescence spectra differ significantly from the spectra calculated above for the same experimental conditions (compare Figs. 4 and 10, spectrum 4), even when collisions are taken into account. The ratios of the intensities between separate components in the spectrum are different from the computed ratios, the lines are found to be significantly broadened, and the shifts of the line maxima do not correspond to the generalized Rabi frequencies Ω_j^\pm . The latter circumstance is clearly seen in the detuning $\Delta\lambda_j^\pm = \lambda_j^\pm - \lambda_L$ of the wavelengths $\lambda_j^\pm = 2\pi c/\omega_j^\pm$ of the maxima of the recorded fluorescence components as a function of the detuning $\Delta\lambda_L$, presented in Fig. 11. Figure 11 also shows the detuning, calculated from the quasienergy spectrum of the three-level system according to Eqs. (18) and (19), of the components for intensity 20 MW/cm^2 (curves 3), corresponding to the experimental conditions. As follows from the data presented, the measured positions of the components in the entire range of detuning $\Delta\lambda_L$ are significantly displaced from the computed values and correspond to a much lower intensity $\mathcal{I}=5 \text{ MW/cm}^2$, whose computed curve is also presented in Fig. 11. Moreover, as the experiments showed, the intensity of the laser radiation incident on the resonant medium has virtually no effect on the shifts of the components; this is clearly seen in Fig. 12, which displays the positions of the maxima of the components ω_1^- as a function of the intensity \mathcal{I} . We note that the same figure also displays the curve, calculated from the quasienergy spectrum, of the detuning of the same component versus the intensity of the laser beam. This plot exhibits

significant disagreement from the experimental data, especially for large values of \mathcal{I} .

The experimentally observed modification of the fluorescence spectra accompanying a change in the density of the resonant medium also does not agree with the above theoretical model of the fluorescence of a three-level medium in a strong laser field. It follows from the theoretical calculations that, as in the well-studied case of a two-level medium (see, for example Refs. 4 and 5), even though N significantly influences the shape of the fluorescence spectra and the fluorescence intensity the quasienergy structure of a three-level atom and, correspondingly, the frequencies of the fluorescence components do not depend on the density of the resonance medium. However, the shape of the fluorescence spectrum (Fig. 13) recorded at relatively low sodium vapor densities ($N \approx 2 \cdot 10^{13} \text{ cm}^{-3}$) differs significantly from the measured spectrum with $N \approx 2.3 \cdot 10^{15} \text{ cm}^{-3}$ (Fig. 10, spectrum 4): The ω_2^- fluorescence compo-

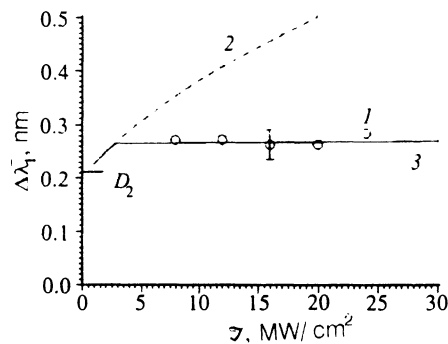


FIG. 12. Experimental (1) and computed (2, 3) detuning $\Delta\lambda_1^-$ of the component ω_1^- as a function of the laser-radiation intensity. The position of the D_2 line of sodium is indicated on the detuning axis. 2—Detuning calculated according to Eqs. (18) and (19) from the Rabi splitting of a three-level system. 3—Detuning calculated taking into account the spatial distribution of the laser beam in the form (23) and absorption in the unperturbed sodium vapors; $\Delta\lambda_L=0.21 \text{ nm}$, $N=4.4 \cdot 10^{14} \text{ cm}^{-3}$.

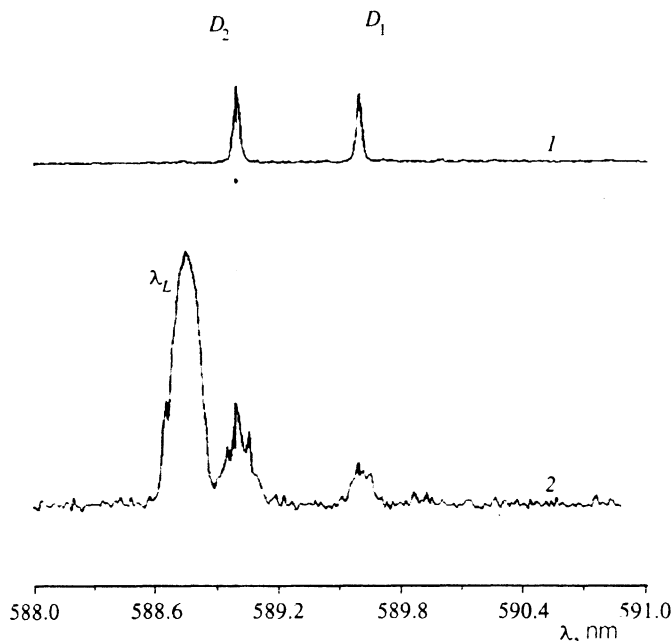


FIG. 13. Experimentally measured fluorescence spectrum (2) in low-density sodium vapor, $N=2 \cdot 10^{13} \text{ cm}^{-3}$, $\Delta\lambda_L=0.21 \text{ nm}$, $\mathcal{I}=20 \text{ MW/cm}^2$. 1—Calibration spectrum of the sodium lamp.

ment vanishes and the maxima of the ω_1^- and ω_3^- lines shift toward the position of the unperturbed D_1 and D_2 lines of sodium (the lines in the spectrum shown in Fig. 13 are somewhat wider than the data in Fig. 10 because the input slit of the spectrograph must be much wider in order to record a weak fluorescence signal under the low-density conditions of the resonance medium). The displacement of the maximum of the ω_1^- component as a function of N is also clearly seen in Fig. 14, where these data are displayed.

Note that the multicomponent structure of the fluorescence spectra of sodium vapors is observed under the conditions of the present experiment only if the intensity of the exciting laser radiation is significant. Figure 15 displays the intensities of separate fluorescence components, integrated over their spectrum, as a function of \mathcal{I} for $\Delta\lambda_L=0.21 \text{ nm}$. It is evident from the plots in the figure that as the intensity of the laser beam decreases, the intensity of the ω_2^- component, which originates from interference of the $3^2P_{1/2}$ and $3^2P_{3/2}$ states of the sodium atom, primarily decreases rapidly in the fluorescence spectrum. Here we do not consider the ω_2^+ and ω_3^+ components, which are weak even for quite high values of \mathcal{I} . The ω_3^- component practically vanishes, and among the displaced components only ω_1^+ and ω_1^- remain, i.e., the fluorescence acquires a purely two-level character.

6. NUMERICAL MODELING OF FLUORESCENCE IN A THREE-LEVEL MEDIUM UNDER REAL EXPERIMENTAL CONDITIONS

The observed discrepancy between the computed and experimentally measured fluorescence spectra could be caused by several factors. On the one hand, the transverse spatial nonuniformity of the laser beam, as a result of which the generalized Rabi frequency Ω_j' is also spatially nonuniform, could affect both the experimentally measured shifts of the fluorescence components and their spec-

tral width. In addition, because the fluorescence saturates for large values of \mathcal{I} the spatial wings of the laser beam, where the radiation intensity is relatively low, will make a significant contribution to the shape of the recorded spectra. On the other hand, absorption of fluorescence photons in dense sodium vapors which are not disturbed by the laser radiation distorts the measured spectra, and simple

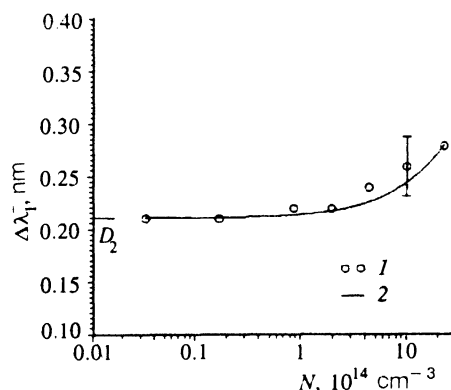


FIG. 14. Detuning $\Delta\lambda_1^-$ of the ω_1^- component as a function of the sodium vapor density measured experimentally (1) and computed (2), taking into account the spatial distribution of the laser beam in the form (23) and absorption in the unperturbed vapors. The position of the D_2 line of sodium is indicated on the detuning axis; $\Delta\lambda_L=0.21 \text{ nm}$, $\mathcal{I}=20 \text{ MW/cm}^2$.

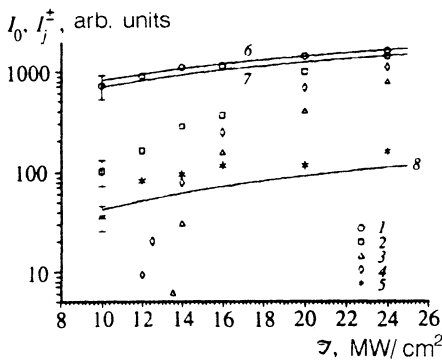


FIG. 15. Intensities I_j^\pm of the fluorescence components as a function of the laser-radiation intensity. Experimentally measured (1–5) and computed (6–8), taking into account the spatial distribution of the laser beam in the form (23) and absorption in the unperturbed vapors; $\Delta\lambda_L=0.21$ nm, $N=4.4 \cdot 10^{14}$ cm $^{-3}$. 1, 6—intensity of the fluorescence component at the laser frequency; 2, 7—intensity of the ω_1^- component; 3— ω_2^- ; 4— ω_3^- ; and 5, 8— ω_1^+ .

estimates show that the distortion can be very large, even though the frequencies of the components are detuned from resonance considerably. Aside from this, the phase self-modulation of the laser radiation is also found to be significant. The influence of this modulation is manifested especially in the broadening of the unsaturated component of the fluorescence at the laser frequency. It should be noted, however, that time-resolved experiments would enable us to eliminate, when recording the fluorescence, the change in the generalized Rabi frequency Ω_j' during the laser pulse and the displacement of the fluorescence lines toward the unperturbed transition frequencies in the vapor afterglow.

In order to give a quantitative interpretation of our experimental results we used the basis of the theoretical model described above, to perform time-independent numerical calculations of the fluorescence spectra of sodium vapor in the three-level approximation, taking into account the strongest effects which result in deformation of the observed spectra—spatial nonuniformity of the laser beam and absorption of fluorescence photons in sodium vapors not disturbed by the laser radiation. Once again, in modeling the spectra we employed the buffer-gas collision broadening constants and the resonance broadening constants presented in Refs. 18–20.

The laser intensity distribution $\mathcal{I}(r)$, required for numerical modeling of real fluorescence spectra, was found over the cross section of the laser beam by least-squares fitting of the experimentally measured beam profile (presented in Fig. 7) by different functional forms. The calculations showed that the optimum representation (giving the smallest rms deviation from the measured profile) is achieved by representing the beam profile by a Lorentzian with an exponent of 1.5:

$$\mathcal{I}(r) = \mathcal{I}_0 [r_0^2 / (r^2 + r_0^2)]^{1.5}, \quad (23)$$

represented by trace 2 in Fig. 7. We note that a spatial distribution of the same form was employed in Ref. 5 in

order to approximate the experimentally measured beam profile. For comparison the figure also displays the approximation of the distribution $\mathcal{I}(r)$ by a Gaussian function (curve 3):

$$\mathcal{I}(r) = \mathcal{I}_0 \exp(-r^2/r_0^2). \quad (24)$$

According to the data presented in the figure, as compared to the Gaussian profile the Lorentzian function gives a significantly better description of the beam profile for small r and, more important, though not as noticeable, a better description of the relatively even dropoff of the intensity distribution at the beam periphery.

Since the laser beam is cylindrically symmetric, the experimentally measured spectral intensity $J(\lambda)$ of the scattered radiation per unit length is determined by the spectrum of scattered photons taking into account propagation effects. Its wavelength dependence is given by

$$J(\lambda) \propto \iint A[\lambda, \mathcal{I}(r), r] \times \exp\left(-\int_0^{|r-r_0|} \sigma[\lambda, N(r'), \mathcal{I}(r')] N(r') dr'\right) \times d|r-r_0| dr_\varphi d\Omega, \quad (25)$$

where $\sigma[\lambda, N(r'), \mathcal{I}(r')]$ is the radiation absorption cross section or, possibly, in some spectral ranges also the gain—in the case of propagation in a region where a strong laser field is present (see Secs. 2 and 3, as well as Refs. 11 and 22). The integral in the expression (25) extends over rays which connect the scatterer and the radiation detector, whose coordinates are r and r_0 , respectively, with respect to the laser-beam axis. The integral over Ω describes the solid angle within which the scattered radiation is collected by the receiver, and the integral over the coordinate r_φ describes the summation of fluorescence from atoms located on the arcs of a circle with radius r . The integration over the coordinate r' describes the absorption (or amplification) of fluorescence photons propagating from the scattering atom to the radiation detector. Note that the effect of reabsorption in the undisturbed vapor is neglected, since the fluorescence spectra were measured synchronously with excitation of the medium by the laser pulse, whose duration is only slightly longer than the radiative decay time—16 nsec.²⁸

Analysis of the expression (25) shows that it can be significantly simplified, since propagation effects over the cross section of the laser beam can be neglected in the region occupied by the beam. This is associated with the small radius of the laser beam and bleaching of the medium due to saturation effects. For this reason $J(\lambda)$ can be expressed as follows:

$$J(\lambda) \approx J_0(\lambda) K(\lambda), \quad (26)$$

where $J_0(\lambda)$ is the spectral intensity of the fluorescence emitted by the excitation region in the direction of the radiation detector and $K(\lambda)$ describes the effective absorption of fluorescence photons propagating through the region of undisturbed atoms.

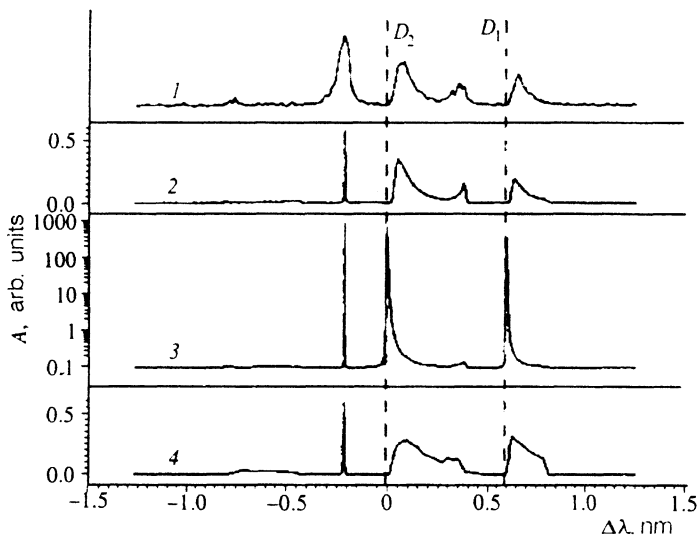


FIG. 16. Measured (1) and computed (2-4) fluorescence spectra of sodium vapors with detuning $\Delta\lambda_L=0.21$ nm; $N=2.3 \cdot 10^{15}$ cm $^{-3}$, $\mathcal{I}=20$ MW/cm 2 . 2—Calculation taking into account the spatial distribution $\mathcal{I}(r)$ in the form (23) as well as absorption in the unperturbed sodium vapors; 3—calculation taking into account the spatial distribution $\mathcal{I}(r)$ in the form Eq. (23) neglecting absorption in the unperturbed sodium vapors; 4—calculation with $\mathcal{I}(r)$ in the form (24) taking into account absorption in the unperturbed sodium vapors.

The shape of the fluorescence spectrum $J_0(\lambda)$ determined by the nonuniformity of the laser beam was calculated by integrating the expression (11) obtained in Sec. 2 over the beam cross section, taking into account the wavelength dependence of the fluorescence intensity distribution $A[\lambda, \mathcal{I}(r)]$ on the intensity of the laser radiation:

$$J_0(\lambda) \propto (\theta/4\pi) \int_0^{2\pi} d\varphi \int_0^\infty A[\lambda, \mathcal{I}(r)] r dr, \quad (27)$$

where θ is the solid angle within which the fluorescence of the vapor is recorded.

The spectrum computed in this manner for the conditions of Fig. 10 (spectrum 4) and the intensity distribution $\mathcal{I}(r)$ in the form of the Lorentzian (23) is shown in Fig. 16 (curve 3). As follows from this figure, all components of the spectrum, with the exception of the fluorescence line at the laser wavelength, are found in this case to be significantly broadened (as is observed experimentally), but the ratio of their intensities and the positions of the maxima once again disagree with the observations. A characteristic feature of the computed spectrum in this case is the displacement of the maxima of the ω_1^- and ω_3^- components toward the frequencies of the unperturbed D_1 and D_2 transitions. This is connected with the fact that for a Lorentzian distribution $\mathcal{I}(R)$ a significant fraction of the laser energy from the wings of the distribution has a low intensity, and in these regions the generalized Rabi frequencies Ω_1 and Ω_3 are essentially equal to the detuning Δ_3 and Δ_2 from resonance (see Sec. 2). At the same time, because fluorescence saturates for large \mathcal{I} the extended wings of the distribution $\mathcal{I}(R)$ will make the dominant contribution to the total fluorescence intensity, and this will displace the maxima of the spectra of the components toward the resonance frequencies. Moreover, the peak intensity \mathcal{I}_0 in the distribution (23), as the calculation showed, does not change the shape of the spectrum; it merely increases the total intensity. As far as the undisplaced component ($\omega=\omega_L$) is concerned, it remains narrow and is not visible on the scale of the figure, since its position, naturally, is not influenced by variations of the laser intensity.

As discussed previously, two components—elastic and inelastic—contribute to the intensity of the undisplaced component (see also, for example, Ref. 2). Since the multifrequency nature of the exciting radiation and the finite resolution of the monochromator were neglected in the calculations, the computed width of the inelastic component is found, once again, to be of the order of the collisional width. However, the calculations show that the contribution of the elastic component to the fluorescence spectrum is once again small because of the strong effect of collisions under the conditions of the present experiment.

Subsequent calculations showed that good agreement with the experimental data can be obtained only by taking into account the absorption of fluorescence photons in the region of sodium vapor which is not perturbed by the laser radiation. In the present work the effective absorption $K(\lambda)$ was calculated taking into account the measured density profile $N(R)$ of the resonant medium (see Fig. 9):

$$K(\lambda) = \exp \left[- \int_0^{R_0} \sigma[\lambda, N(R)] N(R) dR \right], \quad (28)$$

where $R_0 \approx 5$ cm is the radius of the sodium vapor column. In calculating the absorption cross section $\sigma[\lambda, N(R)]$ we have included the explicit dependence of the relaxation constants on the sodium vapor density at different points along the radius of the cell. In calculations of $K(\lambda)$ only the Lorentzian (homogeneous) broadening of the absorption line was taken into account, since when the detuning from the unperturbed absorption line, which actually influences the fluorescence line profile, is large it is easy to show that the Doppler broadening can be neglected. The computed fluorescence spectrum, obtained by multiplying the spectrum $J_0(\lambda)$ by the quantity $K(\lambda)$, is shown in Fig. 16 (spectrum 2) for $\Delta\lambda_L=0.21$ nm, and as follows from the plots it agrees well with the experimentally observed spectrum, which is also plotted in the same figure for convenience. When absorption is taken into account, the fluorescence near the D lines is practically completely trapped by the unperturbed sodium vapor. This results in a displacement of the maximum of the spectral components

ω_1^- and ω_3^- into the intermediate region falling between the detuning from the corresponding line and the generalized Rabi frequency, as is observed experimentally. As a result, the intensities of the components ω_1^- and ω_2^- are also found to be of the same order of magnitude, though when absorption was neglected they differed significantly from one another (compare the spectra 2 and 3 in Fig. 16).

As the laser intensity changes, the spectral dependence of the absorption $K(\lambda)$ naturally does not change, and as mentioned above the computed fluorescence line shape also does not change. For this reason, for example, as long as the quantity $\Omega'_1 - \Delta_3$ (for the conditions of Fig. 16) remains greater than the characteristic spectral width $\Delta\lambda_{ab}$ in the absorption region, the position of the maximum of the component ω_1^- (see Fig. 12, curve 3) calculated from Eq. (26) does not depend on \mathcal{I} ; this is confirmed by the experimental data. Decreasing the vapor density reduces the absorption and the characteristic width $\Delta\lambda_{ab}$; this displaces the components ω_1^- and ω_3^- in the direction of resonance (Fig. 14, curve 2) and also agrees with experiment. It is important, however, that agreement with the experimental data is found only for a Lorentzian intensity profile $\mathcal{I}(r)$ —see Eq. (23). Thus Fig. 16 (curve 4) displays the computed fluorescence spectrum for a Gaussian profile $\mathcal{I}(r)$, which describes the experimentally recorded spectrum significantly less well. This is manifested, in particular, in the almost complete merging of the components ω_1^- and ω_2^- and is connected with the rapid decay of the intensity at the periphery of the laser beam for the distribution (24). In this connection we emphasize that the intensity profile $\mathcal{I}(r)$ was determined in the experiments in the absence of sodium vapor. For sufficiently high vapor density the profile of an intense laser beam can be effectively broadened due to excitation of four-wave instability.¹¹⁻¹³ This will result in more even decay of the intensity on the wings of the distribution. Due to the saturation of the resonant medium, however, the compression of the laser beam as a result of large-scale self-focusing, which occurs when $\lambda_L < \lambda_{D_2}$, is apparently insignificant under the present experimental conditions.

In analyzing our experimental data we are struck by the fact that the fluorescence intensity does not saturate with increasing laser radiation intensity (see Fig. 15). This effect has been noted many times and discussed in many works (see, for example, Refs. 5 and 20). Note that under our conditions with significant detuning of the laser wavelength from the resonance wavelength the saturation intensity \mathcal{I}_s , though it is very high (it is easy to show that $\mathcal{I}_s \approx 2 \text{ MW/cm}^2$ for $\Delta\lambda_L = 0.21 \text{ nm}$ and $N = 2.3 \cdot 10^{15} \text{ cm}^{-3}$), is significantly lower than the experimentally achieved laser intensities $\mathcal{I} \approx 25 \text{ MW/cm}^2$, and this gives grounds for expecting saturation of the fluorescence intensity. Huennekens and Gallagher²⁰ were the first to suggest that the gradual saturation of the resonant medium at the periphery of the laser beam is responsible for the fact that fluorescence is not saturated with increasing laser beam intensity; this has been confirmed by a series of indirect experimental data and simple calculations. Since, however, in Ref. 20 the laser radiation was tuned to resonance with

the atomic transition, under high-absorption conditions the nonsaturation effect was associated with “burning through” the resonance medium. Under the conditions of the present work, for significant detuning $\Delta\lambda_L$ from resonance there was virtually no attenuation of the laser radiation in the sodium vapor. This enables us to investigate in pure form the dependence of the fluorescence intensity on the intensity of the laser beam. Our calculations of the dependence of the intensities of the separate fluorescence components on \mathcal{I} , the results of which are also presented in Fig. 15, show that Huennekens and Gallagher’s supposition²⁰ that the wings of the spatial distribution of the laser radiation intensity play an important role in fluorescence nonsaturation is correct. In order to match the theoretical curves with the experimental data the computed dependence of the fluorescence line strength at the laser frequency I_0 was normalized to its value obtained in the experiment with $\mathcal{I} = 20 \text{ MW/cm}^2$. According to the data presented in Fig. 15 the theoretical curves describe well the behavior of the intensities I_0 and I_1^+ of the components of the fluorescence spectrum. The agreement between the theoretical curve for I_1^- and experiment is, however, much worse, especially for low intensities. This is in all probability associated with the shift in the frequency of this component at low intensities \mathcal{I} into the region where the detuning from the resonance line is small. In addition, even a small error in the measured radial distribution of the vapor density in the cell can strongly influence the computed intensity of this component, since the absorption coefficient depends exponentially on N .

It should be noted, however, that besides the indicated role of the peripheral regions of the laser beam in the appearance of nonsaturation of fluorescence, the excitation of the four-wave instability in an intense laser field,¹¹⁻¹³ which can amplify the spontaneously emitted photons even in a direction perpendicular to the axis of the laser beam, can also influence the effect.

7. CONCLUSIONS

Thus in this work for the first time we have obtained the fluorescence spectra of a dense three-level medium in an intense laser field and we have recorded the multicomponent structure of the spectra which is associated with the Rabi splitting of the ground state and the two excited $3P$ levels of the sodium atom into six quasilevels. The experimentally observed asymmetry of the fluorescence spectra is determined by collisions on the one hand and the fundamental multilevel nature of the experimental atomic system on the other. The calculations of the spectra made in this work, taking into account the spatial distribution of the intensity over the beam cross section and the absorption of fluorescence photons in the unperturbed sodium vapor, agree well with the experimental data. Nonetheless, it should be noted that the question of whether or not the time-independent approach is completely applicable in calculations of fluorescence under the conditions of the present experiment remains open.

The present approach to the investigation of resonance fluorescence spectra makes it possible to study not only the

fundamental questions of nonlinear optics and laser spectroscopy, but also provides a method for investigating in practice the optical characteristics of gaseous media. For example, the relaxation constants and, especially, the excitation transfer constant between the upper levels can be measured, since the ratios of the heights of the peaks in the fluorescence spectra depend significantly on the values of these parameters over a wide range.

In conclusion, we wish to express our deep appreciation to D. V. Gaidarenko for helpful discussions of the results and A. V. Brazhnikov for assisting in the experiments.

¹W. Heitler, *The Quantum Theory of Radiation*, Clarendon Press, Oxford, 1954.
²B. R. Mollow, *Phys. Rev.* **188**, 1969 (1969).
³S. G. Rautian and I. I. Sobel'man, *Zh. Eksp. Teor. Fiz.* **41**, 456 (1961) [*Sov. Phys. JETP* **14**, 328 (1962)].
⁴B. R. Mollow, *Phys. Rev. A* **15**, 1023 (1977).
⁵J. L. Carlsten, A. Szoke, and M. G. Raymer, *Phys. Rev. A* **15**, 1029 (1977).
⁶F. Shuda, C. R. Stroud, and M. J. Hercher, *J. Phys. B* **7**, L198 (1974).
⁷W. Harting, W. Rasmussen, R. Shieder, and H. Walther, *Z. Phys. A* **278**, 205 (1976).
⁸R. Grove, F. Wu, and S. Ezekiel, *Phys. Rev. A* **15**, 227 (1977).
⁹A. G. Leonov, A. A. Pantelev, V. N. Starostin, and D. I. Chekhov, *Pis'ma Zh. Eksp. Teor. Fiz.* **58**, 959 (1993) [*JETP Lett.* **58**, 895 (1993)].
¹⁰M. O. Scully and W. E. Lamb, *Phys. Rev.* **159**, 208 (1967).
¹¹D. V. Gaidarenko, A. G. Leonov, A. A. Pantelev, A. N. Starostin, and D. I. Chekhov, *Laser Phys.* **3**, 151 (1993).

¹²A. G. Leonov, A. A. Pantelev, V. N. Starostin, and D. I. Chekhov, *Pis'ma Zh. Eksp. Teor. Fiz.* **55**, 228 (1992) [*JETP Lett.* **55**, 223 (1992)].
¹³D. V. Gaidarenko, A. G. Leonov, A. A. Pantelev, V. N. Starostin, and D. I. Chekhov, *Kvant. Elektron.* **19**, 1001 (1992) [*Sov. J. Quantum Electron.* **22**, 931 (1992)].
¹⁴B. R. Mollow, *Progress in Optics XIX*, 1981, p. 3.
¹⁵E. V. Baklanov, *Zh. Eksp. Teor. Fiz.* **65**, 2203 (1973) [*Sov. Phys. JETP* **38**, 1100 (1974)].
¹⁶M. Sargent III, D. A. Holm, and M. S. Zubary, *Phys. Rev. A* **31**, 3112 (1985).
¹⁷S. Stenholm, D. A. Holm, and M. Sargent III, *Phys. Rev. A* **31**, 3124 (1985).
¹⁸R. H. Chatham, A. Gallagher, and E. L. Levis, *J. Phys. B* **13**, L7 (1980).
¹⁹C. G. Carrington, D. M. Stacey, and J. Cooper, *J. Phys. B* **6**, 417 (1973).
²⁰J. Huennekens and A. Gallagher, *Phys. Rev. A* **28**, 238 (1983).
²¹E. G. Pestov, *Trudy FIAN* **187**, 60 (1988).
²²B. R. Mollow, *Phys. Rev. A* **5**, 2217 (1972).
²³N. B. Delone and V. P. Krainov, *Atoms in Strong Fields*, Springer, N. Y., 1985.
²⁴H. R. Zaidi, *Can. J. Phys.* **59**, 737 (1981).
²⁵A. A. Pantelev, V. A. Roslyakov, A. N. Starostin *et al.* *Zh. Eksp. Teor. Fiz.* **97**, 1777 (1990) [*Sov. Phys. JETP* **70**, 1003 (1990)].
²⁶L. V. Keldysh, *Zh. Eksp. Teor. Fiz.* **47**, 1515 (1964) [*Sov. Phys. JETP* **26**, 1018 (1965)].
²⁷M. A. Cappelli, P. G. Cardinal, H. Herchen, and R. M. Measures, *Rev. Sci. Instrum.* **56**, 2030 (1985).
²⁸A. A. Radtsig and B. M. Smirnov, *Reference Data on Atoms, Molecules, and Ions*, Springer, Berlin (1985).

Translated by M. E. Alferieff